Onset of Area-Dependent Dissipation in Droplet Spreading

Mark Ilton,[1] Oliver Bäumchen,[2] and Kari Dalnoki-Veress[1,3,*]
[1]Department of Physics and Astronomy and the Brockhouse Institute for Materials Research, McMaster University, Hamilton, Ontario L8S 4M1, Canada
[2]Max Planck Institute for Dynamics and Self-Organization (MPIDS), 37077 Göttingen, Germany
[3]Laboratoire de Physico-Chimie Théorique, UMR CNRS 7083 Gulliver, ESPCI ParisTech, PSL Research University, Paris, France
(Received 16 January 2015; revised manuscript received 27 May 2015; published 22 July 2015)

We probe the viscous relaxation of structured liquid droplets in the partial wetting regime using a diblock copolymer system. The relaxation time of the droplets is measured after a step change in temperature as a function of three tunable parameters: droplet size, equilibrium contact angle, and the viscosity of the fluid. Contrary to what is typically observed, the late-stage relaxation time does not scale with the radius of the droplet—rather, relaxation scales with the radius squared. Thus, the energy dissipation depends on the contact area of the droplet, rather than the contact line.

DOI: 10.1103/PhysRevLett.115.046103 PACS numbers: 68.08.Bc, 47.55.D-, 68.15.+e, 82.35.Gh

The dynamics of a liquid wetting a solid substrate has applications in diverse technologies including oil recovery [1], coating deposition [2], electronic paper [3], capillary switches [4], and microfluidics [5]. Flow in liquids can be driven by a number of forces (e.g., gravity, surface tension, external electromagnetic fields), which are mediated by inertial and viscous forces in the fluid. Large inertial forces can lead to oscillatory motion [6–17], whereas viscous forces cause damping. The study of the viscous (i.e., low Reynold's number) motion of wetting fluids has been the focus of much research because it is typically dominant at the micrometer and nanometer length scales (for reviews see Refs. [18–23]), and it is the subject of the current Letter. For a viscous liquid droplet that wets a substrate there are two possible cases: complete wetting and partial wetting depending on the presence and interplay of short- and long-ranged intermolecular forces in the system [24]. In the case of complete wetting, the final equilibrium state is that of a flat liquid film of uniform thickness covering the substrate. The dynamics of this process is well understood in both the case of an initially dry substrate [24,25], as well as the case where the substrate is covered by a prewetted film of the same liquid [26]. On the other hand, in partial wetting the final equilibrium state is a droplet that makes a well-defined equilibrium contact angle θ_e with the substrate [24]. In this case, the dynamics of a droplet as it moves towards equilibrium is less well understood and there are unresolved fundamental questions [21], in particular involving the nature of energy dissipation as a droplet spreads.

Exponential relaxation is a generic feature of near-equilibrium partial wetting, having been observed in capillaries [27,28], droplet coalescence [29–31], stripe spreading [32], and droplet spreading [30,33–35]. For a system with a well-defined volume Ω the relaxation time τ of the exponential decay is a function of Ω, θ_e, and the fluid viscosity η. In the limit of small contact angles, there are several different predictions for $\tau(\Omega, \theta_e, \eta)$ [32,34–39], but there is a dearth of experimental systems where τ can be systematically probed as a function of all three variables. The lack of experiments is largely due to the fact that contact angle pinning is the bane of careful dynamics measurements especially at small contact angles [40] and can occur at even dilute concentrations of defects [41].

Here, we use a liquid-substrate system that allows the systematic probing of partially wetting droplets that coexist with a nanoscopically thin layer of the same liquid (known as pseudopartial wetting [42,43]), as shown schematically in Fig. 1(a). Droplets with a well-defined θ_e coexisting in equilibrium with a prewetted layer can arise from a single global minimum (or even multiple minima in the case of stratified films [44]) of the effective interface potential, i.e., the free energy of the system comprising repulsive and attractive intermolecular interactions. Little is known about the dynamics of moving contact lines in the partial wetting regime with a prewetting layer [45]. The dynamics depends on whether there is enough material to fully prewet the substrate [46,47], and previous measurements of liquids in a capillary subjected to a pressure difference saw no evidence of contact line pinning in the case of a prewetting layer, a problem that is common in partial wetting [45].

The system investigated here has negligible contact angle hysteresis [44] and is ideally suited to probe the exponential relaxation of droplets near equilibrium. The lack of hysteresis results from the self-assembly of the droplets on a metastable wetting layer of the same material (rather than defect prone manual preparation). We use a lamellar-forming diblock copolymer that dewets into droplets with a quantized spectrum of contact angles. While the details of the quantized droplet system can be found in our earlier study [44], we recall some of the salient features crucial to this work. The diblock copolymer liquid can self-assemble into stacks of monolayers below the

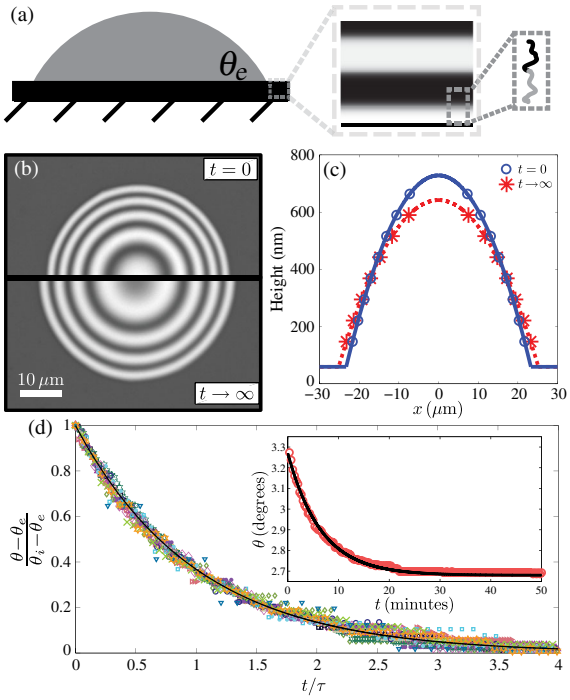

FIG. 1 (color online). (a) Schematic of a mostly disordered droplet, coexisting with an ordered wetting layer of the same liquid. (b) Interference optical microscopy images showing the relaxation of a droplet as it spreads. (c) Best fit spherical cap to the data points from the interference fringes of the droplet in (b) at $t = 0$ (solid line) and at equilibrium as $t \to \infty$ (dashed line). The height scale is exaggerated as compared to the lateral scale for clarity. (d) Normalized relaxation of the contact angle of 15 different representative droplets with different Ω and θ_e, which undergo both advancing and receding motion. The solid line is the function $\exp(-t/\tau)$. The inset shows the relaxation of the contact angle of the droplet from (b) and (c) as a function of time with an exponential fit (black line).

order-disorder transition temperature T_{ODT}, whereas order is destroyed above T_{ODT}. In our experiments we work above T_{ODT}; however, the substrate-liquid and air-liquid interactions have a tendency to induce local ordering. Thus, one can arrange the temperature of the experiment such that a mostly disordered "bulklike" droplet coexists with a wetting layer made up of a stack of monolayers [see the schematic in Fig. 1(a)]. The wetting layer thickness h_e and temperature T determine the free energy of the wetting layer. As a result, the droplet contact angle depends on h_e and T. An increase in T reduces the order in the wetting layer, resulting in a smaller θ_e, and the droplet spreads. Similarly, a decrease in T causes a droplet to recede. Because a change in temperature shifts θ_e, we can examine both advancing and receding droplet motion in a controlled manner simply by performing a step change in the temperature. Thus, we are able to systematically vary Ω, θ_e, and η using a single liquid on a homogeneous substrate with no chemical modification. By measuring the relaxation time of droplets as they approach equilibrium, one can probe the nature of energy dissipation in the droplets.

Previous work has shown that in the case of a simple liquid droplet on a substrate with a small contact angle the majority of the energy dissipation occurs near the contact line, where there is the greatest shear [20]. For late-stage relaxation, the instantaneous contact angle θ exponentially decays to θ_e with a relaxation time [20,38,48] (see the Supplemental Material [49])

$$\tau_L \propto \frac{\eta}{\gamma}\frac{\Omega^{1/3}}{\theta_e^{10/3}}, \tag{1}$$

where γ is the liquid-air surface tension. To probe the energy dissipation in a structured liquid and the role of the prewetting layer, we examine the near-equilibrium ($\theta \approx \theta_e$) dynamics of droplets. We will show that, in contrast with the assumptions made leading to Eq. (1), the relaxation of the droplets is consistent with a contact area dependent dissipation mechanism being dominant.

As described previously [44], thin films of polystyrene-poly(2 vinyl pyridine) (PS-P2VP) diblock copolymer were spincast onto silicon wafers from a dilute solution of toluene at slow speeds to purposefully create films of nonuniform thickness (the PS-P2VP was obtained from Polymer Source Inc., Canada, $M_n = 16.5$ kg/mol with an equal block composition). Upon heating above $T_{\mathrm{ODT}} = 160\,^{\circ}\mathrm{C}$ the liquid dewets into droplets coexisting with ordered wetting layers. The contact angle of the droplets was measured from Newton rings using optical microscopy with a monochromatic filter (460 nm) as shown in Fig. 1(b) [26]. A relaxation measurement was performed as follows. The sample temperature is controlled using a high-precision ($\pm 0.1\,^{\circ}\mathrm{C}$) heating device (Linkam, UK). First, a droplet was held at $T = T_i$ until it reached its equilibrium initial contact angle θ_i. At time $t = 0$, the temperature of the system was changed by $10 \pm 0.1\,^{\circ}\mathrm{C}$ to T_f. The temperature equilibrates rapidly (within 10 sec) compared to the measurement time (tens of minutes). $\theta(t)$ was measured until the droplet reached its new equilibrium contact angle θ_e. Figures 1(b)–1(d) show a typical measurement of a droplet with an initial contact angle of 3.29°, just as the temperature is rapidly changed from 180 to 190 °C. The approach to the equilibrium contact angle of $\theta_e = 2.69°$ for this advancing droplet is shown in the inset of Fig. 1(d). Note that both the contact angle and the change in the contact angle are small, validating the small angle and $\theta \approx \theta_e$ approximations.

The relaxation time $\tau(\Omega, \theta_e, \eta)$ of 60 droplets was measured at different T_f (between 180–210 °C) for droplets of varying Ω and coexisting with different h_e (between 5–15 ordered monolayers). An exponential decay well describes the droplet relaxation for both advancing and receding contact angles [Fig. 1(d)]. There is negligible contact angle hysteresis ($< 0.1°$) [44]; thus, θ_e does not depend on whether the droplet is advancing or receding.

The relaxation time, however, does depend on whether the droplet is advancing or receding towards θ_e.

Previous studies [32,34–39] predict that, because the dominant mechanism for dissipation is viscous dissipation near the contact line, $\tau \propto \Omega^{1/3}$ [see Eq. (1)]. The data here, however, are not consistent with this scaling (see Fig. S1 in the Supplemental Material [49]). As the essential assumptions related to the contact angle are safely validated (i.e., $\theta \approx \theta_e < 10°$) and the droplet volume stays constant to within 5% as the droplet spreads, the only possible explanation for the deviation from $\tau \propto \Omega^{1/3}$ is that the assumption of contact line dissipation is wrong. If we write a generalized power dissipation as $\mathcal{P}(r,\theta) \propto K r^{\alpha} \theta^{\beta} \dot{r}^2$, then in the limit of near-equilibrium relaxation to a small θ_e, the contact angle dynamics follows an exponential decay with relaxation time (see the Supplemental Material [49])

$$\tau \propto \frac{K}{\gamma} \frac{\Omega^{\alpha/3}}{\theta_e^{(\alpha/3-\beta+2)}}. \tag{2}$$

In the case of purely viscous dissipation at the contact line, $K = \eta$, $\alpha = 1$, and $\beta = -1$, which recovers the contact line relaxation time of Eq. (1), as required. Here, the diblock copolymer is an anisotropic fluid near the substrate: the wetting layer consists of stacked monolayers and the base of the droplet is also ordered. We might then suspect that the base of the droplet could provide a mechanism for a contact area dependent dissipation. In that case $\alpha = 2$ and $\beta = 0$, resulting in $\tau \propto \Omega^{2/3}$. In Fig. 2(a) we plot τ as a function of $\Omega^{2/3}$ for four different values of T_f. Indeed, we find that the data are consistent with a straight line going through the origin.

For an area-dependent dissipation $\mathcal{P}_A \propto K r^2 \dot{r}(t)^2$ and using Eq. (2), the relaxation time is

$$\tau_A = \frac{\kappa}{\gamma} \frac{\Omega^{2/3}}{\theta_e^{8/3}}, \tag{3}$$

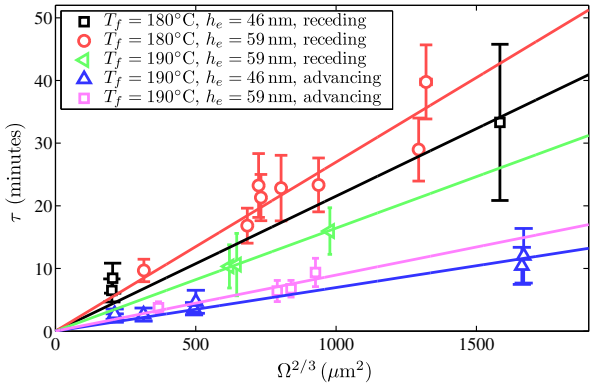

FIG. 2 (color online). The relaxation time τ as a function of $\Omega^{2/3}$ for different values of (T_f, h_e) (with correspondingly different θ_e) as indicated in the legend, for receding and advancing droplet motion. Solid lines are the best fit to a $\tau \propto \Omega^{2/3}$ scaling with zero intercept.

where $\kappa \propto K$. Just as $K = \eta$ for pure viscous dissipation at the contact line, here κ also governs the dynamics. Given $\gamma \approx 31$ mJ/m^2 for the experimental temperatures used [50], and by measuring τ, θ_e, and Ω experimentally, we can obtain κ for each droplet. We find that κ is not a constant, and depends on θ_e as shown in Fig. 3. Furthermore, κ decreases as temperature is increased, and also depends on whether the motion is advancing or receding.

For the diblock copolymer system, the dynamics represented by κ is more complex than η for a simple liquid. The dynamics depends on both the mobility, or friction, of the molecules as well as the degree of segregation of the two blocks within the monolayers. In the limit of an unsegregated wetting layer, the droplet will completely spread ($\theta_e \to 0$) since the wetting layer and droplet would form a homogeneous liquid. As $\theta_e \to 0$, the area-dependent dissipation must also vanish and $\kappa \to 0$ [26]. Conversely, with greater induced order in the monolayers the area-dependent dissipation increases. Since θ_e increases with greater segregation of the wetting layers [44], this means that κ must increase with θ_e. For small θ_e, and to first order, $\kappa \propto \theta_e$, consistent with the linear fits shown as the solid lines in Fig. 3. The molecular mobility at the base of the droplet, while not equivalent to the viscosity due to the presence of order, is still a molecular friction and can be expected to scale with the viscosity, $\kappa \propto \eta(T)$. Thus, we can then write $\kappa = \theta_e \eta / \Lambda$ with Λ a constant with a dimension of length. This gives the area-dependent relaxation time as

$$\tau = \frac{\eta \Omega^{2/3}}{\gamma \theta_e^{5/3} \Lambda}. \tag{4}$$

Our data are consistent with this relationship (Fig. 4). Here, we use $\eta/\gamma = 0.045$ min/μm at 180 °C for PS-P2VP [51], and the Williams-Landel-Ferry scaling of polystyrene [52] to calculate $\eta(T)/\gamma$. To recognize that the droplet relaxation might be different for advancing and receding motion, we allow Λ to differ for advancing Λ_a or receding Λ_r motion.

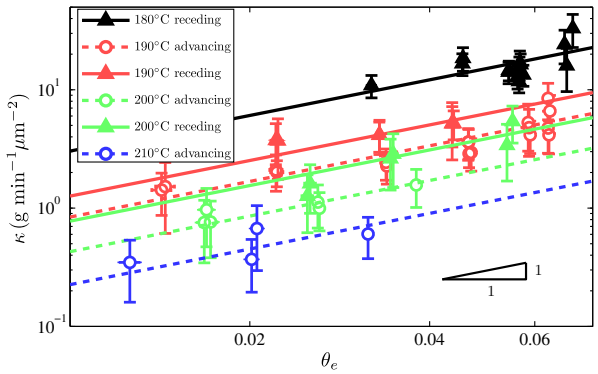

FIG. 3 (color online). The area-dependent relaxation prefactor κ plotted as a function of θ_e (shown on a double logarithmic plot for clarity of the data). κ is not a universal constant for the system, and depends on T as well as θ_e. The lines are fit to $\kappa \propto \theta_e$.

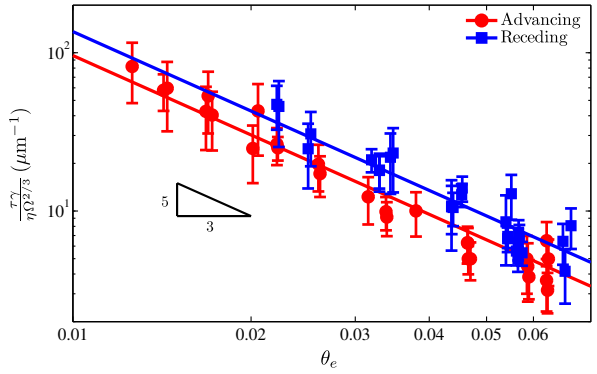

FIG. 4 (color online). The normalized relaxation time as a function of the final contact angle for advancing (circles) and receding (squares) contact line motion. The lines are the best fit of Eq. (4) to the data, with $\Lambda_a = 22 \pm 1$ μm and $\Lambda_r = 16 \pm 1$ μm.

The difference in Λ_a and Λ_r indicates that relaxation is faster for advancing than for receding when comparing droplets with the same Ω and θ_e. This result can be easily understood as follows. In a typical experiment the droplet radius changes by approximately 15%. For a given Ω and θ_e, receding droplets have a greater base area during the course of their evolution, resulting in a stronger power dissipation and slower relaxation times. We note that the ratio $\Lambda_a/\Lambda_r = 1.4$ roughly corresponds to the ratio of the average receding droplet area to the average advancing droplet area given the same volume and final contact angle.

The lack of contact angle pinning in this system has facilitated measurements of the relaxation of a structured liquid droplet in the partial wetting regime. A contact area dependent dissipation describes the data within error using only two adjustable parameters Λ_a and Λ_r. In previous work on the spreading of disordered diblock copolymer droplets in the absence of a prewetted film, a power law consistent with Tanner's law and proportional to $\Omega^{1/3}$ was observed [53]. Thus, a purely viscous dissipation mechanism dominates in the limit of no prewetted film for this system. In contrast, the experimental results show the onset of a secondary dissipation mechanism that is area dependent and originates from the presence of the ordered wetting layer.

The origin of the area-dependent dissipation could be from the onset of a hydrodynamic slip boundary condition at the base of the droplet, i.e., a nonzero horizontal velocity of the fluid at the interface [54]. Interfacial slip has previously been observed in a manifold of different systems, ranging from small molecule liquids, e.g., *n*-alkanes [55], which can have a prewetted layer similar to the system studied here [56], to large molecule liquids like polymers. In particular, slippage of polymeric liquids has been subjected to extensive theoretical and experimental studies (see Ref. [57] and the references therein), including slip at polymer-polymer interfaces in multilayered films [58]. The dissipated power of a slip mechanism due to friction at a fluid interface scales with the contact area between the moving fluid and the substrate, in contrast to viscous dissipation, which predominantly acts in the immediate vicinity of the contact line [24]. In thin polymer films dewetting from hydrophobic substrates, it is precisely the area dependence of the slip mechanism that has been shown to govern the growth dynamics of holes [57,59,60] as well as the appearance of characteristic instabilities of receding liquid fronts [61]. Thus, our observations on the area-dependent droplet relaxation dynamics are consistent with interfacial slip between the (disordered) droplet and the (well-ordered) wetting layer.

The onset of a hydrodynamic slip boundary condition could be the result of the structure of the diblock copolymer molecules near the interface and an anisotropy in their dynamics [62,63]. In a previous molecular dynamics study, the degree of hydrodynamic slip was shown to be related to the microscopic structure induced by the interfaces of a thin fluid film [64]. This idea has also been supported by experimental findings on the interfacial molecular structure of polymeric liquids that exhibit a significant amount of slip [65]. In the case of droplet dynamics, as the droplet spreads its height decreases to conserve volume, and this flow perpendicular to the layers would be hindered by the anisotropy in the dynamics leading to an apparent interfacial slip between successive layers of fluid.

In summary, we have measured the relaxation time of droplets of a structured liquid in the pseudopartial wetting regime as a function of three tunable parameters, droplet volume, equilibrium contact angle, and viscosity, $\tau = \tau(\Omega, \theta_e, \eta)$. For the first time, we are able to vary these parameters on the same sample leading to quantitatively comparable measurements. The diblock copolymer used provides a robust system for the measurement of contact angle dynamics because there is negligible pinning of the contact line ($< 0.1°$). The ideal nature of this system is the direct result of the pseudopartial wetting regime: rather than manually preparing droplets on an ideal surface, the droplets can self-assemble on a metastable wetting layer of the same material. In all 60 experiments we observe that the droplet relaxation scales with the base area of the droplet. This is in direct contrast with the spreading of simple liquids where the energy is dissipated near the contact line of the droplet, and scales with the radius. The area-dependent dissipation can be interpreted as arising from the presence of anisotropic molecular dynamics leading to an apparent interfacial slip.

The authors would like to thank NSERC (Canada) and the German Research Foundation (DFG) under Grant No. BA 3406/2.

*dalnoki@mcmaster.ca

[1] A. Paterson, M. Robin, M. Fermigier, P. Jenffer, and J. Hulin, J. Pet. Sci. Eng. **20**, 127 (1998).

[2] T. D. Blake, A. Clarke, and K. J. Ruschak, AIChE J. **40**, 229 (1994).
[3] R. A. Hayes and B. J. Feenstra, Nature (London) **425**, 383 (2003).
[4] A. H. Hirsa, C. A. López, M. A. Laytin, M. J. Vogel, and P. H. Steen, Appl. Phys. Lett. **86**, 014106 (2005).
[5] C. Cottin-Bizonne, J.-L. Barrat, L. Bocquet, and E. Charlaix, Nat. Mater. **2**, 237 (2003).
[6] K. Stoev, E. Ramé, and S. Garoff, Phys. Fluids **11**, 3209 (1999).
[7] L. M. Hocking and S. H. Davis, J. Fluid Mech. **467**, 1 (2002).
[8] A.-L. Biance, C. Clanet, and D. Quéré, Phys. Rev. E **69**, 016301 (2004).
[9] A. L. Yarin, Annu. Rev. Fluid Mech. **38**, 159 (2006).
[10] P. M. McGuiggan, D. A. Grave, J. S. Wallace, S. Cheng, A. Prosperetti, and M. O. Robbins, Langmuir **27**, 11966 (2011).
[11] X. Zhang and O. A. Basaran, J. Colloid Interface Sci. **187**, 166 (1997).
[12] A. Prosperetti, Phys. Fluids **24**, 032109 (2012).
[13] S. Ramalingam, D. Ramkrishna, and O. A. Basaran, Phys. Fluids **24**, 082102 (2012).
[14] J. B. Bostwick and P. H. Steen, Phys. Fluids **21**, 032108 (2009).
[15] O. A. Basaran, J. Fluid Mech. **241**, 169 (1992).
[16] J. C. Bird, S. Mandre, and H. A. Stone, Phys. Rev. Lett. **100**, 234501 (2008).
[17] J. B. Bostwick and P. H. Steen, Annu. Rev. Fluid Mech. **47**, 539 (2015).
[18] T. D. Blake, J. Colloid Interface Sci. **299**, 1 (2006).
[19] D. Bonn, J. Eggers, J. Indekeu, J. Meunier, and E. Rolley, Rev. Mod. Phys. **81**, 739 (2009).
[20] P.-G. de Gennes, Rev. Mod. Phys. **57**, 827 (1985).
[21] J. Ralston, M. Popescu, and R. Sedev, Annu. Rev. Mater. Res. **38**, 23 (2008).
[22] J. H. Snoeijer and B. Andreotti, Annu. Rev. Fluid Mech. **45**, 269 (2013).
[23] M. Ramiasa, J. Ralston, R. Fetzer, and R. Sedev, Adv. Colloid Interface Sci. **206**, 275 (2014).
[24] P.-G. de Gennes, F. Brochard-Wyart, and D. Quéré, *Capillarity and Wetting Phenomena: Drops, Bubbles, Pearls, Waves* (Springer, New York, 2004).
[25] L. Tanner, J. Phys. D **12**, 1473 (1979).
[26] S. Cormier, J. McGraw, T. Salez, E. Raphaël, and K. Dalnoki-Veress, Phys. Rev. Lett. **109**, 154501 (2012).
[27] R. Cox, J. Fluid Mech. **168**, 169 (1986).
[28] Y. Suo, K. Stoev, S. Garoff, and E. Ramé, Langmuir **17**, 6988 (2001).
[29] C. Andrieu, D. A. Beysens, V. S. Nikolayev, and Y. Pomeau, J. Fluid Mech. **453**, 427 (2002).
[30] R. Narhe, D. A. Beysens, and V. S. Nikolayev, Langmuir **20**, 1213 (2004).
[31] D. A. Beysens and R. D. Narhe, J. Phys. Chem. B **110**, 22133 (2006).
[32] G. McHale, C. V. Brown, and N. Sampara, Nat. Commun. **4**, 1605 (2013).
[33] F. Rieutord, O. Rayssac, and H. Moriceau, Phys. Rev. E **62**, 6861 (2000).
[34] M. Härth and D. Schubert, Macromol. Chem. Phys. **213**, 654 (2012).
[35] M. D. Ruijter, J. D. Coninck, and G. Oshanin, Langmuir **15**, 2209 (1999).
[36] J. Radulovic, K. Sefiane, and M. E. R. Shanahan, J. Phys. Chem. C **114**, 13620 (2010).
[37] R. Chebbi, J. Adhes. Sci. Technol. **25**, 1767 (2011).
[38] G. McHale, M. I. Newton, and N. J. Shirtcliffe, J. Phys. Condens. Matter **21**, 464122 (2009).
[39] T. Roques-Carmes, V. Mathieu, and A. Gigante, J. Colloid Interface Sci. **344**, 180 (2010).
[40] E. Pérez, E. Schäffer, and U. Steiner, J. Colloid Interface Sci. **234**, 178 (2001).
[41] M. Reyssat and D. Quéré, J. Phys. Chem. B **113**, 3906 (2009).
[42] F. Brochard-Wyart and P.-G. de Gennes, Adv. Colloid Interface Sci. **34**, 561 (1991).
[43] P. Silberzan and L. Leger, Phys. Rev. Lett. **66**, 185 (1991).
[44] M. Ilton, P. Stasiak, M. W. Matsen, and K. Dalnoki-Veress, Phys. Rev. Lett. **112**, 068303 (2014).
[45] L. Du, H. Bodiguel, C. Cottin, and A. Colin, Chemical Engineering and Processing **68**, 3 (2013).
[46] L. Leger and P. Silberzan, J. Phys. Condens. Matter **2**, SA421 (1990).
[47] F. Brochard-Wyart, J. D. Meglio, D. Quéré, and P.-G. de Gennes, Langmuir **7**, 335 (1991).
[48] G. McHale, S. Rowan, and M. Newton, J. Phys. D **27**, 2619 (1994).
[49] See Supplemental Material at http://link.aps.org/supplemental/10.1103/PhysRevLett.115.046103 for a derivation of the contact angle scaling laws.
[50] B. B. Sauer and G. T. Dee, Macromolecules **35**, 7024 (2002).
[51] R. D. Peters and K. Dalnoki-Veress, Eur. Phys. J. E **37**, 100 (2014).
[52] P. Lomellini, Polymer **33**, 4983 (1992).
[53] A. B. Croll and K. Dalnoki-Veress, Eur. Phys. J. E **29**, 239 (2009).
[54] C. L. M. F. Navier, Mem. Acad. Sci. Inst. Fr. **6**, 389 (1823).
[55] J.-H. Cho, B. M. Law, and F. Rieutord, Phys. Rev. Lett. **92**, 166102 (2004).
[56] P. Lazar, H. Schollmeyer, and H. Riegler, Phys. Rev. Lett. **94**, 116101 (2005).
[57] O. Bäumchen and K. Jacobs, J. Phys. Condens. Matter **22**, 033102 (2010).
[58] P. C. Lee, H. E. Park, D. C. Morse, and C. W. Macosko, J. Rheol. **53**, 893 (2009).
[59] C. Redon, J. Brzoska, and F. Brochard-Wyart, Macromolecules **27**, 468 (1994).
[60] R. Fetzer and K. Jacobs, Langmuir **23**, 11617 (2007).
[61] O. Bäumchen, L. Marquant, R. Blossey, A. Münch, B. Wagner, and K. Jacobs, Phys. Rev. Lett. **113**, 014501 (2014).
[62] T. P. Lodge and M. C. Dalvi, Phys. Rev. Lett. **75**, 657 (1995).
[63] A. B. Croll, M. W. Matsen, A.-C. Shi, and K. Dalnoki-Veress, Eur. Phys. J. E **27**, 407 (2008).
[64] P. A. Thompson and M. O. Robbins, Phys. Rev. A **41**, 6830 (1990).
[65] P. Gutfreund, O. Bäumchen, R. Fetzer, D. van der Grinten, M. Maccarini, K. Jacobs, H. Zabel, and M. Wolff, Phys. Rev. E **87**, 012306 (2013).